Original Article

Decellularized xenogenic bone graft for repair of segmental bone defect in rabbits

Tamilmahan, P.[1*]; Pathak, R.[2]; Rashmi,[1]; Amarpal,[2]; Aithal, H. P.[2]; Mohsina, A.[1]; Tiwari, A. K.[3] and Karthik, K.[4]

[1]Ph.D. Student in Veterinary Surgery and Radiology, Division of Veterinary Surgery, Indian Veterinary Research Institute, Izatnagar, Bareilly, Uttar Pradesh, India; [2]Division of Veterinary Surgery, Indian Veterinary Research Institute, Izatnagar, Bareilly, Uttar Pradesh, India; [3]Division of Biological Standardization, Indian Veterinary Research Institute, Izatnagar, Bareilly, Uttar Pradesh, India; [4]Department of Veterinary Microbiology, TANUVAS, Tamil Nadu, India

[*]***Correspondence:*** *P. Tamilmahan, Resident Veterinary Service Section, Madras Veterinary College, Chennai, Tamil Nadu-600007, India (current address). E-mail: drtamilmahan.bison@gmail.com*

10.22099/IJVR.2022.40785.5906

(Received 25 May 2021; revised version 21 Jul 2022; accepted 22 Aug 2022)

Abstract

Background: Bone grafting is a preferred treatment option for the healing of large diaphyseal bone defects and is useful in the management of nonunion, delayed union, and tumor resection. **Aims:** To investigate a decellularization protocol of bovine cancellous bone for xenogenic implantation in radial bone defects in rabbits. **Methods:** Bovine bone scaffolds fabricated with various decellularization protocols viz phosphate buffer saline (PBS), 1% sodium dodecyl sulfate (SDS), and rapid freeze and thaw technique. The manufactured scaffolds were characterized by biomechanical testing, histological staining, and scanning electron microscopy. A 10 mm rabbit radius bone defect was repaired with autograft and SDS treated and rapid freeze and thaw in groups A, B, and C respectively. Healing was evaluated by radiography and histopathology at 0, 30, 60, and 90 days. The grafts were also checked for host tissue reaction and incorporation into the defect. **Results:** The freeze and thaw group showed complete elimination of all cellular nuclei, regular arrangement of collagen fiber, and no significant difference in tensile strength compared to 1% SDS treated and native groups. The *in vivo* radiographic and histopathological study showed that the rapid freeze and thaw group had complete bridging of the bone gap defect with new bone formation and they were immunologically less reactive compared to group B. **Conclusion:** The *in vitro* and *in vivo* evaluation of the grafts suggested that freeze and thaw technique was most superior to all other techniques for effective decellularization and augmentation of bone healing with better integration of the graft into the host.

Key words: Bovine bone graft, Bone defect, Bone regeneration, Decellularization, Rapid freeze and thaw

Introduction

Bone grafting is a preferred treatment option for the healing of large diaphyseal bone defects and is useful in the management of nonunion, delayed union, and arthrodesis. Conditions such as tumor resection, cyst, or high-energy trauma may lead to the formation of large bone defects that must be filled with a graft to regain original function as quickly as possible (Jonitz *et al*., 2011). Autograft, allograft, and xenograft have been used clinically as graft substitutes (Mollon *et al*., 2013). However, their frequent use may be hampered by several impediments such as limited availability, donor site morbidity, the possibility of infection transmission, and graft rejections (Kalab *et al*., 2015). Though several synthetic and natural graft materials have been evaluated for bone grafting, the quest for a bioresorbable, easy to handle, mechanically strong, free from pathogens, and cost-effective bone scaffold still continues (Kalab *et al*., 2015). Among the available choices, a xenogenic bone graft may satisfy most of the requirements of the graft material as its unlimited supply, osteoconductive, cost-effectiveness and biodegradable properties make it suitable as a bone substitute in orthopedic and dental surgery. Among various available sources of xenogenic graft, bovine bones are most commonly used for orthopedic treatment (Stievano *et al*., 2008; Quan *et al*., 2014). The most important obstacle to the use of xenogenic graft is the recognition of the graft as a foreign antigen leading to overt immune-mediated rejection of the graft (Oryan *et al*., 2014). It is believed that decellularization of graft tissue using specific agents can effectively remove the xenogenic antigens, cellular, and nuclear materials without altering the composition, biological activity, or mechanical integrity of the remaining extracellular bone matrix (ECM) (Badylak *et al*., 2011). The molecules that remain in the ECM are conserved across the species line and can be accepted by the xenogenic recipient (Gock *et al*., 2004). For instance, FDA approved the use of acellular dermal matrix for

various clinical applications. Scaffolds derived from naturally occurring ECM have been used in tissue engineering applications. The present study was undertaken to investigate a different method of decellularization of bovine cancellous bone for xenogenic implantation in radial bone defects in rabbits.

Materials and Methods

Preparation of decellularized bovine cancellous bone

Full-length femur bones from five buffaloes of 1.5-2 years of age were collected aseptically from an abattoir within 3 h of slaughtering. Cylindrical bone pieces measuring 20 × 20 mm^2 were cut from the metaphyseal region of each bone using an osteotome. The bone pieces were washed with high-velocity stream water to remove the marrow from the pore spaces. The bone explants were kept for 1 h in phosphate buffer saline (PBS) with 0.1% ethylenediamine tetraacetic acid (EDTA) (Sigma Aldrich, USA) at room temperature (Fröhlich *et al*., 2010). Thereafter, the bone explants were assigned randomly into three different treatment groups each consisting of 10 explants. The explants of the first group (group A) were immersed in PBS for 24 h and kept as control. The second group (group B) explants were immersed in 250 ml of decellularization solutions containing 1% sodium dodecyl sulfate (w/v) (SDS) (Sigma Aldrich, USA) in a 500 ml capacity beaker. Both groups were agitated at 1 g on a horizontal shaker plate for 24 h at 25°C. After decanting the decellularization solution, the bone explants were washed with PBS solution 5 times within a period of 1 h to remove the residual chemicals and stored at -20°C. In the third group (group C), the explants were exposed to 5 freeze-thaw cycles. For each time, the bone explants were put into a metal beaker containing liquid nitrogen for 1 min and thawed at 56°C for 5 min.

The bone explants of each group were then put into enzymatic solutions containing 0.5 mg/ml DNase 1, 50 µg/ml RNAse (Merck Bioscience), 0.02% EDTA, and 1% Penicillin/Streptomycin/Fungizone (P/S/F), in PBS for 3 h at 37°C with agitation to remove any remaining cellular material (Elder *et al*., 2009). After decanting the enzymatic solution, the bone grafts were washed 5 times in PBS solution for 1 h. The bone grafts were then air dried and exposed to UV irradiation for 2 h in a UV chamber. Finally, the grafts were stored in 0.15 M PBS (pH 7.4) at -20°C for further use.

Evaluation of decellularized bone

Histological analysis

The decellularized bone specimens were fixed in neutral buffered 10% formalin. Before sectioning, the specimens were decalcified in a solution containing 5 ml of nitric acid, 5 ml of formaldehyde (38-42%), and 40 ml of distilled water, and embedded in paraffin blocks. The sections were stained with haematoxylin and eosin (H&E) stain to evaluate cellular contents. Special staining for collagen was done using Masson's trichrome stain (MT), and safranin O stain was used for glycosaminoglycans content (GAG).

DNA quantification

DNA extraction was done by conventional phenol/chloroform DNA extraction procedure (Sambrook and Russell, 2001) after crushing the bone pieces into powder. The DNA content was quantified using a nanodrop spectrophotometer.

Scanning electron microscopy

Tissue constructs were washed in PBS, and fixed in 2.5% glutaraldehyde in PBS overnight at 4°C. The samples were washed three times with 0.1 M cacodylate buffer (Sigma-Aldrich, USA) in 1 M hydrogen chloride (Sigma-Aldrich, USA), pH 7.4, and dehydrated in a series of ethanol solutions (Merck, Germany). Then, the tissue samples were dried in a Critical Point Dryer (JEOL, Japan) using CO_2 as the transitional fluid. After that, Specimens were mounted on aluminium stubs using adhesive silicon tape and subjected to a thin layer of gold/palladium ion sputtering using the Jeol ion sputter (JFC 1600, Japan) at 7-10 mA and 1-2 kV for 15 min. Finally, the processed specimens were observed under a scanning electron microscope (JEOL, JSM 6610 LV, Japan) at appropriate acceleration voltage and magnification range to identify the collagen fiber orientation and surface architecture (Chan *et al*., 2013).

Mechanical tests

The tensile properties of different decellularized scaffolds were determined by a uniaxial material testing system (ADMET. INC MA 02062, USA) with a 100 Kilo Newton (KN) load. The samples were cut into 20 mm × 40 mm for tensile testing, and into 10 mm × 20 mm to perform compression tests. Tensile specimens were glued into pre-aligned brass end caps with a dental acrylate mixture. For each construct, the stiffness (Young modulus of elasticity) was calculated as the slope of the linear portion of the load-deformation curve using spreadsheet program. The specimens were randomly assigned to tension and compression studies (Lee *et al*., 2016).

Implantation of the decellularized graft

The Institute Animal Ethics Committee (IAEC) approved the study. Twenty-seven clinically healthy New Zealand white rabbits (*Oryctolagus cuniculus*) of either sex were randomly divided into 3 groups consisting of 9 animals each. A standard 10 mm defect was created in all the rabbits left mid radial diaphysis under anesthesia due to the administration of xylazine (6 mg/kg) and ketamine (60 mg/kg) (Amarpal *et al*., 2010) (Figs. 1A-C). The segmental defect was filled by autogenous bone in group A (control) and by the same size of decellularized bone grafts viz, group B (SDS), and group C (freeze and thaw). Postoperatively, the treated limbs were stabilized with bamboo splints.

Fig. 1: The Acellular bone graft implanted in rabbit radius defect. (**A**) Marked 1 cm defect in diaphysis of radius bone, (**B**) 1 cm gap defect, and (**C**) The defect filled with acellular bone graft

Plain radiography

Radiographs of the defect site were made after surgery and subsequently on 30, 60, and 90 days postoperatively. Radiographs were interpreted for the status of the implanted scaffold, new bone formation, the extent of callus, and bridging of the gap according to a modified X-ray scoring system (Heiple *et al*., 1987; Lane and Sandhu, 1987) (Table 1).

Histological analysis

All the samples were collected and decalcified in Goodling Stewart's solution after the humane method of euthanizing using thiopentone sodium on days 30, 60, and 90 (3 animals for each interval). The tissues were processed in a routine paraffin embedding manner and 4 µm thick sections were cut and stained with H&E stain. Bone healing was assessed in each group using a modified histopathological scoring system (Heiple *et al*., 1987; Lane and Sandhu, 1987) (Table 1).

Immunological studies

Lymphocyte stimulation test

The cell-mediated immune response toward decellularized xenogenic bone graft was assessed by performing a lymphocyte stimulation test as reported by Kruisbeek *et al*. (2004). The free protein content of native as well as decellularized bone grafts was estimated by Lowry's method for the preparation of antigens. The cell-mediated immune response was assessed by MTT (3-(4,5-dimethylthiazol-2-yl)-2,5-diphenyltetrazolium bromide) colorimetric assay. Blood (2 ml) was aseptically collected from the orbital sinus of the rabbit in heparinized tubes on 0, 22, 42, and 62 post-implantation days. An equal volume of sterile PBS was added to the collected blood and mixed properly. The mixture was layered over 2 ml of lymphocyte separation medium (Histopaque 1077, Sigma Aldrich, USA) and was centrifuged at 400 g for 30 min. The buffy coat was collected in a fresh tube and washed twice with sterile PBS at 300 g for 10 min. The supernatant was discarded and the pellet was resuspended in RPMI 1640 growth medium (GM) (Gibco, USA). The cells were adjusted to a concentration of 2×10^6 viable cells/ml in RPMI 1640 and 100 µL of resuspended cells were seeded in each well of a 96-well plate. The cells were incubated at 37°C in a 5% CO_2 environment. Cells from each rabbit were stimulated in triplicates with native bone antigen (10-20 µg/ml) and phytohaemagglutinin (10 µg/ml) (Sigma Aldrich, USA), a T-cell mitogen, and three wells were left unstimulated as negative controls. After 45 h, 40 µL of MTT solution (5 mg/ml) was added to each well and incubated further for 4 h in 5% CO_2 environment. The plates were then centrifuged for 15 min in plate centrifuge at 800 g. The supernatant was discarded, plates were dried and 150 µL DMSO was added to each well and mixed thoroughly by repeated pipetting to dissolve the formazan crystals. The plates were immediately read at 570 nm, with 620 nm as a reference wavelength. The stimulation index (SI) was calculated using the following formula:

Stimulation index (SI) = Optical density (OD) of stimulated cultures/OD of unstimulated cultures

Indirect ELISA

Optimization of antigen and antibody concentration was done using a hyperimmune serum standard curve. The preimmune (day 0) serum sample was used as negative control and 60th day sample was used as a positive control for plotting the standard curve.

Around 1 ml of blood was collected from the orbital sinus of the test animals at 0, 7, 14, 28, 42, 62, and 82 days in sterile vials. Antigen at a concentration of 20 µg/well in coating buffer (pH 9.6) was coated in the 96-well flat bottom polystyrene plate (Nunc MaxiSorp®) and incubated at 4°C overnight in a humidified chamber. The plates were washed three times with PBS plus 0.05% Tween 20 (PBS-T). The unbound sites of the wells were blocked by adding 5% skimmed milk powder in a blocking buffer (200 µL/well) for 2 h at 37°C. After washing, the plates were incubated at 37°C for 1.5 h with 100 µL of diluted serum samples in PBS (1:10) containing 5% skimmed milk powder. After another washing, 100 µL goat anti-rabbit immunoglobin G conjugated with peroxidase (diluted 1:15000), added to

each well (Sigma-Aldrich, St. Louis, USA), and incubated at 37°C for 1 h. Finally, the unbound conjugates were washed thoroughly with washing buffer, and the color reaction was developed by adding 100 µL of freshly prepared tetramethyl benzidine solution to each well and incubating at room temperature for 30 min in dark. The reaction was stopped by 50 µL of 3 M sulphuric acid for each well, and the intensity of color reaction was recorded at 450 nm using an ELISA reader. The values were plotted graphically to obtain a standard curve that is used for the determination of antibody amounts in the samples. The values of antibody titer were expressed in ng/ml (Remya *et al*., 2014).

Table 1: Modified Heiple *et al*. (1987) and Lane and Sandhu (1987) radiological and histopathological scoring system

S. No.	Description	Score
I	**Radiological scoring**	
1	Reduction in defect size	
	Less than 25% reduction	1
	25-50% reduction	2
	50-75% reduction	3
	More than 75% reduction	4
	No gap	5
2	Radiographic density	
	No density	0
	Slight	1
	Moderate	2
	Dense	3
3	Remodeling of bone	
	No remodeling	0
	Less than 25% reduction in size of callus	1
	25-50% reduction in size of callus	2
	50-70% reduction in size of callus	3
	More than 75% reduction in size of callus and canalization of marrow cavity	4
4	Maximal possible radiological score	12
II	**Histopathological scoring**	
1	Union	
	No evidence of union	0
	Fibrous union	1
	Osteochondral union	2
	Bony union	3
	Complete organization of shaft	4
2	Marrow	
	None is resected area	0
	Beginning to appear	1
	Present in more than half of the defect	2
	Complete colonization by red marrow	3
	Mature fatty marrow	4
3	Cancellous bone	
	No osseous cellular activity	0
	Early apposition of new bone	1
	Active apposition of new bone	2
	Reorganizing cancellous bone	3
	Complete reorganization of cancellous bone	4
4	Cortical bone	
	None	0
	Early appearance	1
	Formation under way	2
	Mostly reorganized	3
	Completely formed	4
5	Total point possible per category	
	Osteogenesis	4
	Union	4
	Marrow	4
	Cancellous bone/medullary bone	4
	Cortical/compact bone	4
	Total histological score	16

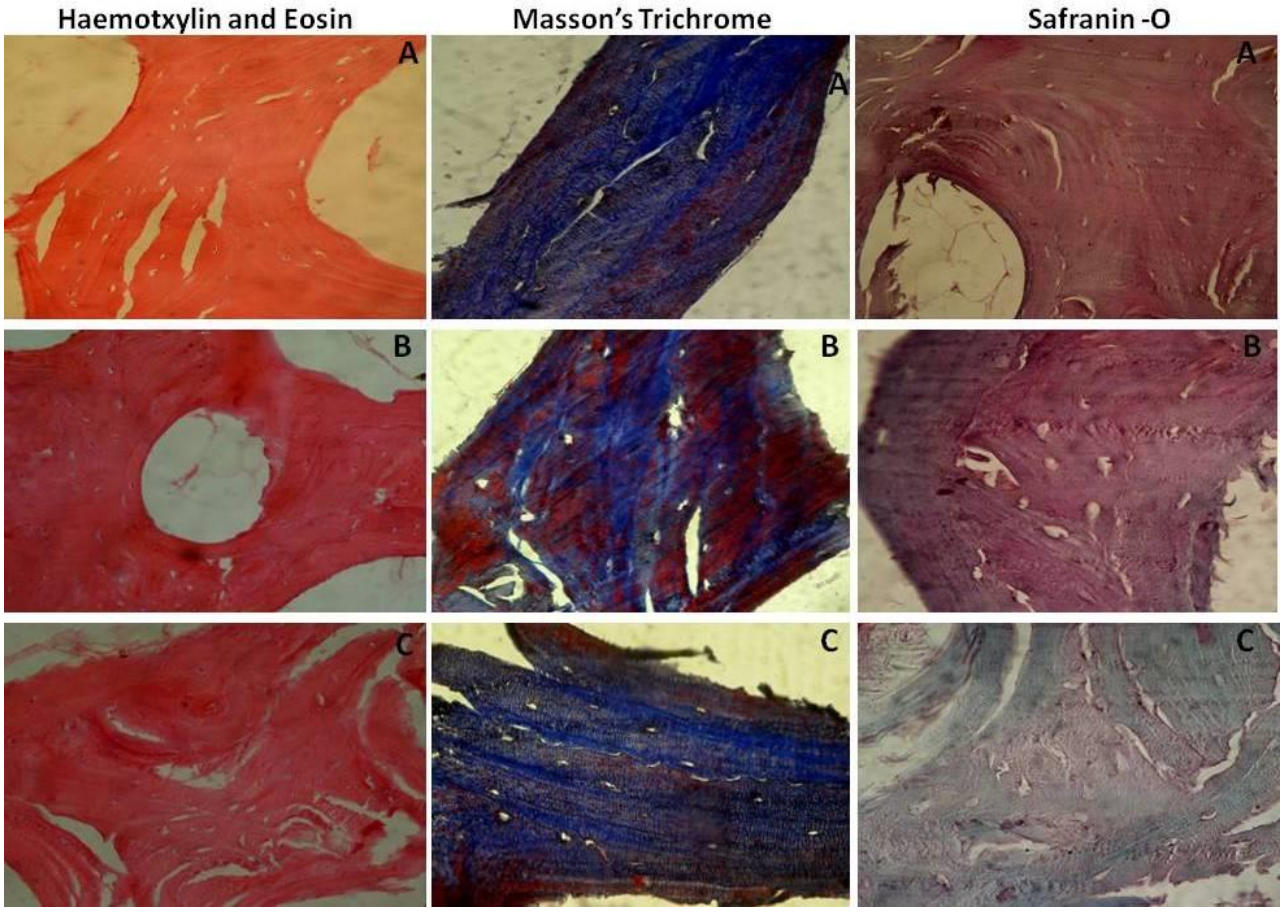

Fig. 2: Photomicrographs demonstrating construct cellularity. Native bone, SDS, and F&T (H&E staining; **A**, **B**, and **C**), collagen fiber arrangement Masson trichrome stain (MT; **A**, **B**, and **C**) and glycosaminoglycan content (GAG) safranin O stain (**A**, **B**, and **C**) (original magnifications ×40)

Statistical analysis

The data were analyzed by using the SPSS statistical software (Illinois, USA, version 16) and the results were expressed as mean±SD. Parameters of different decellularization methods were compared using non-parametric ANOVA followed by Tukey's post hoc test. A value of $P<0.05$ was considered statistically significant.

Results

Histological evaluation

The control bone explants showed more number of osteocytes with nuclei in the osteoid matrix (Fig. 2A, H&E). Slight reduction of cell numbers was seen in the SDS-treated group (Fig. 2B, H&E). In the freeze and thaw treated group, the complete removal of cells with empty porous osteoid matrix was noticed (Fig. 2C, H&E). The bundles of collagen fibers of the freeze-thaw group were regular and tightly packed as in the native tissue. Whereas, in the SDS group, the collagen fibers were irregular and thin (Figs. 2A-C, MT). The intensity of glycosaminoglycans (GAGs) was more in the native and SDS groups. While, the freeze and thaw group showed fewer GAGs in the Safranin-O stain (Figs. 2A-C, Safranin O).

DNA quantification

Native bone treated with PBS showed a significantly higher concentration of DNA ($P<0.05$) (185.58 ± 42.67 ng/µL) compared to the other two methods of decellularization (Fig. 3). The bone treated with rapid freeze/thaw method showed the lowest values (13.81 ± 3.93) of DNA among the groups, which was significantly lower than that in the SDS group (35.18 ± 7.60).

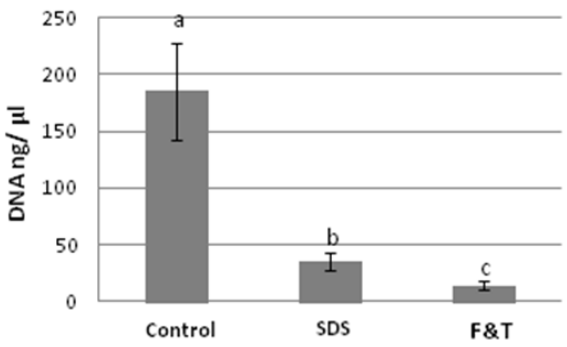

Fig. 3: Total DNA quantification analysis demonstrated freeze and thaw had significantly less DNA content than the SDS group after decellularization

Scanning electron microscopy (SEM)

The collagen fibers in native cancellous bone were disorganized and appeared as a complex network, with fibers intercrossing between layers (Fig. 4A). A similar pattern was found in the bones decellularized with SDS, but the collagen fibers orientation was a little different than that in the control group (Fig. 4B). The fibers of the bone decellularized with rapid freeze and thawing technique appeared to be more regularly packed and less disordered, and even thin fibers were detected (Fig. 4C).

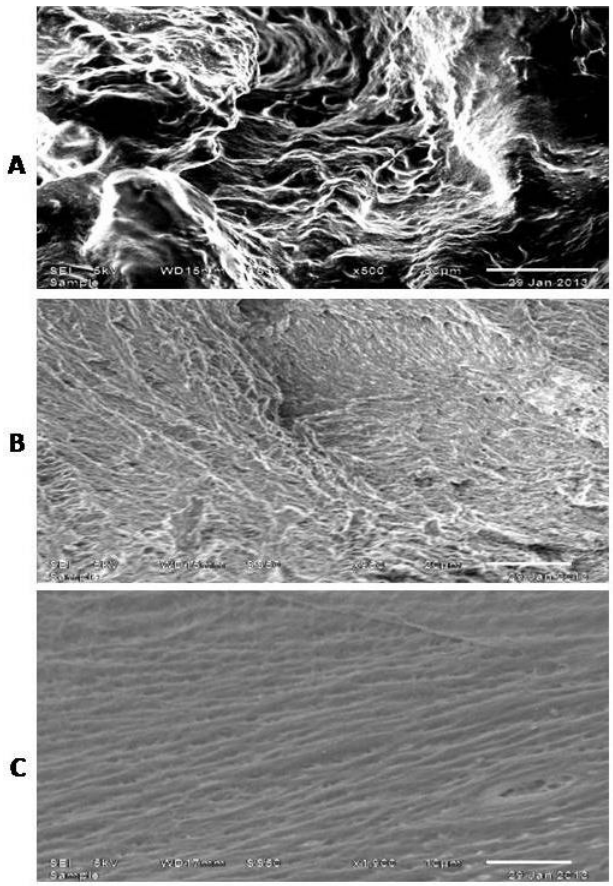

Fig. 4: SEM images of bone construct showing disorganised complex network of collagen fibers in native bone (**A**), more crimped and wavy orientation of collagen fibers of the SDS treated bone (**B**), and densely packed and less disordered collagen fibers in the freeze and thaw group (**C**)

Mechanical tests

The SDS treated bone samples showed the most tensile stiffness, although it was not significantly different from the native and the freeze/thaw groups (P>0.05). Tensile stiffness of control, SDS, and freeze/thaw groups were recorded at 984 ± 166.3 MPa, 1178 ± 313.2 MPa, and 1131 ± 175.4 MPa, respectively.

The values of compressive stiffness results revealed that there was no statistically significant difference between the native and freeze/thaw group (P>0.05). Whereas the SDS treated group showed significantly lesser compressive stiffness compared to the native and freeze/thaw groups (P<0.05). The values of compressive stiffness for the native, SDS and freeze/thaw groups were 722 ± 146 MPa, 285 ± 56.5 MPa, and 545 ± 22.8 MPa, respectively.

Clinical signs

The surgical wound of all animals healed without any signs of inflammation except in group B. Wherein 5 out of 9 animals showed tissue necrosis at the graft site two weeks after surgery, they were excluded from the study. Excluded animals were replaced with new animals in group B. All the animals of three groups showed lameness in the immediate postoperative period but later started to bear weight on the operated limb.

Radiographic observations

On day 0, the defect was clearly visible and filled by a radiopaque acellular scaffold, that looked relatively lesser dense than the adjacent bone in all the groups (Figs. 5A-C). On day 30, the scores of the reduction in gap defect size was significantly higher in groups A and C than those of group B (P<0.05) (Table 2). The radiographic density at the defect site increased in all animals on day 30, but callus was minimal in groups B and C. The moderate periosteal reaction was clearly observed at this stage in groups A and C whereas in group B it was mild.

On day 60, the union of the bone defect was higher (50-60%) in groups A and C, compared to that of group B. However the bridging of bone gap defect in group C (2.33 ± 0.52) was significantly more than that in group B (1.00 ± 0.00) (P<0.05). The score for the reduction in bone defect size in group C was close to the autograft

Table 2: Radiographic (mean±SD) total scores of various parameters in 3 groups (A-C). Time intervals (30, 60, and 90 days), and their interactions

Group and day (interaction)	Reduction in gap	Radiographic density	Remodelling callus	Total score
A × 30	1.44 ± 0.53^{a}	1.22 ± 0.44^{a}	0.00 ± 0.00^{a}	2.67 ± 0.87^{a}
B × 30	0.89 ± 0.33^{b}	1.00 ± 0.00^{a}	0.00 ± 0.00^{a}	1.89 ± 0.33^{b}
C × 30	1.00 ± 0.00^{b}	1.22 ± 0.44^{a}	0.00 ± 0.00^{a}	2.22 ± 0.44^{ab}
A × 60	3.17 ± 0.40^{a}	1.67 ± 0.52^{a}	1.17 ± 0.41^{a}	6.00 ± 0.89^{a}
B × 60	1.00 ± 0.00^{c}	1.00 ± 0.00^{b}	0.33 ± 0.52^{b}	2.33 ± 0.52^{b}
C × 60	2.33 ± 0.52^{b}	1.50 ± 0.55^{a}	0.67 ± 0.52^{ab}	4.50 ± 1.05^{c}
A × 90	5.00 ± 0.00^{a}	3.00 ± 0.00^{a}	3.33 ± 0.58^{a}	11.33 ± 0.58^{a}
B × 90	1.33 ± 0.58^{c}	1.33 ± 0.58^{b}	1.33 ± 0.58^{b}	4.00 ± 0.58^{b}
C × 90	4.00 ± 0.00^{b}	2.33 ± 0.58^{a}	1.68 ± 0.58^{b}	8.00 ± 0.58^{c}

[a, b, c] Means bearing different superscript in a column indicates significant difference (P<0.05) in radiographic score of different grafts on same time interval

Table 3: Histological mean±SD scores of various parameters in 3 groups (A to C). Time intervals (30, 60, and 90 days), and their interaction

Groups	Union	Marrow	Cancellous bone	Cortical bone	Total score
A × 30	2.33 ± 0.58[a]	0.00 ± 0.00	2.00 ± 0.00[a]	1.00 ± 0.00[a]	5.33 ± 0.58[a]
B × 30	0.67 ± 0.58[b]	0.00 ± 0.00	0.67 ± 0.58[b]	0.00 ± 0.00[b]	1.33 ± 1.15[b]
C × 30	2.00 ± 0.00[a]	0.00 ± 0.00	1.33 ± 0.58[ab]	0.00 ± 0.00[b]	3.33 ± 0.58[c]
A × 60	3.00 ± 0.00[a]	1.33 ± 0.58[a]	3.00 ± 0.00[a]	2.00 ± 0.00[a]	9.33 ± 0.58[a]
B × 60	1.33 ± 0.58[b]	0.00 ± 0.00[b]	1.33 ± 0.58[b]	0.67 ± 0.58[b]	3.33 ± 1.15[b]
C × 60	2.33 ± 0.58[a]	0.67 ± 0.58[ab]	2.00 ± 1.00[ab]	1.67 ± 0.58[a]	6.67 ± 1.53[c]
A × 90	3.67 ± 0.58[a]	2.67 ± 0.58[a]	3.33 ± 0.58[a]	2.67 ± 0.58[a]	12.33 ± 2.08[a]
B × 90	1.67 ± 0.58[b]	1.00 ± 0.00[b]	1.67 ± 0.58[b]	1.33 ± 0.58[b]	5.67 ± 0.58[b]
C × 90	3.00 ± 0.00[a]	1.67 ± 0.58[b]	2.33 ± 0.58[b]	2.33 ± 0.58[ab]	9.33 ± 0.58[c]

[a, b, c] Means bearing different superscript in a column indicates significant difference (P<0.05) in radiographic score of different grafts on same time interval

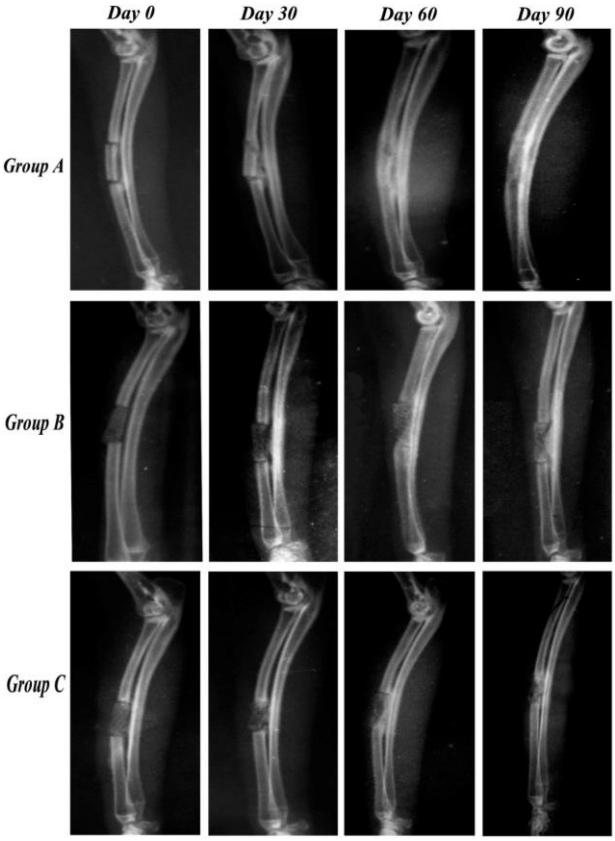

Fig. 5: Mediolateral radiograph of the animals of group **A** (autograft), group **B** (SDS), and group **C** (F&T) showing status of healing at the defect site at different time intervals (0, 30, 60, and 90). Complete bridging of defect site was noticed in group **A** whereas in group **C** healing was yet to complete which stands next to autograft. However, in group **B** still the defect site and radiolucent area was present. Periosteal reaction noticed from the proximal end and ulnar side of defect

(3.17 ± 0.41) (Fig. 5A). The radiographic density in group C was higher as compared to day 30 and close to the autograft on day 60 (Fig. 5C). The radiographic density of group B was significantly lower than those of groups C and A (P<0.05). The periosteal reaction was more intense in group A, moderate in group B, and close to the autograft in group C. Remodelling of the newly formed bone had started at experiment interval in group A, which was indicated by the reduction in the size of the callus, the formation of smooth periosteal callus, and the canalization of medullary cavity due to the absorption of endosteal callus.

The defects were completely filled on day 90; the cortex of the defect along the longitudinal axis was bridged with newly formed bony tissue (Fig. 5A). The mean score for the reduction in defect size was significantly higher in group A (5.00 ± 0.0) and group C (4.00 ± 0.00) than that in group B (P<0.05). Bone healing was minimal in group B rather than other groups (Fig. 5B). The radiographic density of autograft in group A was significantly higher than that in group B (P<0.05), but was not significantly different from that in the group C (Fig. 5C). The remodelling was lagging behind in the animals of groups B and C, and mean remodelling score of the test groups were significantly lower than that of the control group (P<0.01). The periosteal reaction had reduced in the animals of group A whereas it was still present in the animals of other groups.

The total radiographic mean score on day 30 was significantly higher in group A compared to group B but not group C. On days 60 and 90, group A scores were significantly higher than the treatment groups. Among treatment groups, the best healing was observed in group C.

Histological observation

Mean values of a score for different parameters of histological observations in the animals of different groups at 30, 60, and 90 days intervals are presented in Table 3. On day 30, the mean score for the union of bone edges suggested fibrous to osteochondral union that was significantly lower in group B compared to groups A and C (P<0.05). The specimens of group A showed osteochondral union whereas group C showed only fibrous union (Figs. 6A-C). Formation of bone marrow was not evident in any of the groups. The mean score for cancellous bone was significantly higher in group A, compared to groups B and C (P<0.05), whereas in group C it was significantly higher than group B (P<0.05). The cortical bone was not evident in group B (Fig. 6B), while a few animals of groups A and C showed a progression of reorganization of cancellous bone to cortical bone. A comparison between test groups showed higher osteoblastic activity in group C.

On day 60, the union of bone edges was classified as a bony union in the control group (Fig. 6A), and a fibrous to osteochondral union in the treatment groups (Figs. 6B and C). The union of groups A and C was scored significantly ($P<0.05$) higher compared to the group B. The bone marrow formation was the highest in group A, lesser in group C, and the least in group B. The mean scores for cancellous and cortical bone were significantly the highest in group A. The reorganization of cancellous bone to compact bone with red marrow formation in group C was significantly higher compared to group B. In group B, the formation of cancellous bone increased due to higher osteoblastic activity but ossification was minimal compared to other groups.

On day 90, the mean scores for the union of bone gaps also increased in all the groups as compared to these scores on day 60. The score was significantly higher in autograft as compared to group B, but there was no significant difference between groups A and C. The same trend was followed in the marrow, cancellous, and cortical bone formation. The presence of complete red marrow formation with compact bone and at some places, the presence of fatty marrow with complete development of the Haversian system were seen in group A (Fig. 6A). Periosteal fibrous tissue was also visible in group A. In group B, osteolytic changes were visible in the scaffold in two animals. In group C, the complete formation of Haversian system was visible along with compact bone formation (Fig. 6C).

The total histological mean score of group A on all days was significantly higher than that of group C, and the score of group C was significantly higher than that of group B. The best healing response was noticed in group A followed by group C and then group B.

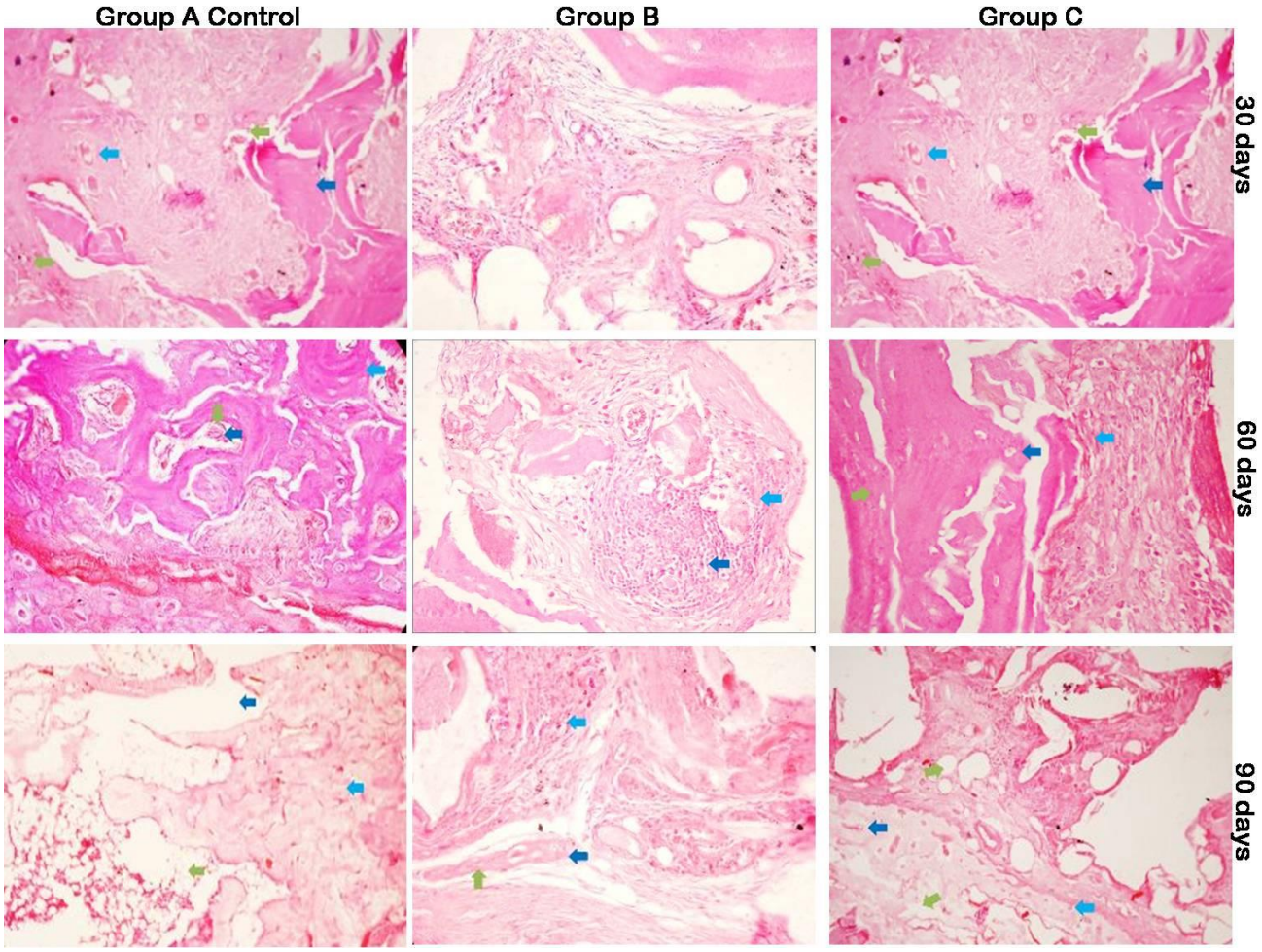

Fig. 6: Photomicrograph showing H&E staining of group **A**, **B**, and **C** under ×40 magnification. Group **A**: On day 30, granulation tissue (healing) (blue arrow) and woven bone formation (dark blue arrow) with osteoid (green arrow) and osteoblasts (green arrow with yellow border). On day 60, the lamellar pattern of bone formation (blue arrow) with prominent osteocytes (dark blue arrow) entrapped in osteoid matrix (green arrow). On day 90, cortical bone formation (blue arrow) and Haversian canal (dark blue arrow) with fatty marrow (green arrow) were evident. Group **B**: On day 30, meagre inflammatory cell accumulation and mild granulation reaction. On day 60, granulation tissue (healing) (blue arrow) with formation of inflammatory cell throngs. On day 90, inflammatory reaction (blue arrow) with bone necrosis (dark blue arrow) and lacunae of dead osteocytes (green arrow). Group **C**: On day 30, the formation of cuboidal and robust juvenile osteoblast (blue arrow) and new bone formation (dark blue arrow) with mild granulation (green arrow). On day 60, bone healing (blue arrow) with osteoid formation (dark blue arrow) as laminae (green arrow). On day 90, cancellous bone (blue arrow) formation with moderate osteoblast population (dark blue arrow) and marrow (green arrow)

Table 4: Mean±SD of stimulation index of rabbits (peripheral blood lymphocytes) treated with acellular antigen on particular graft materials at different time intervals

Groups	Day 0	Day 22	Day 42	Day 62
Group B (SDS)	0.76 ± 0.08^{aA}	1.81 ± 0.03^{bA}	1.94 ± 0.21^{bA}	1.41 ± 0.14^{cA}
Group C (F&T)	0.70 ± 0.07^{aA}	1.48 ± 0.12^{bA}	1.13 ± 0.05^{cB}	0.75 ± 0.00^{aB}

[a, b, c] Means bearing different superscript in a row indicates the significant difference (P<0.05) in the absorbance values at different time interval of particular graft. [A, B] Means bearing different superscript in columns indicates the significant difference (P<0.05) in the absorbance values at same time intervals of in between groups

Table 5: Mean±SD of absorbance values of rabbits (indirect ELISA) treated with different acellular bone graft materials

Group	Day 0	Day 7	Day 14	Day 28	Day 42	Day 62	Day 82
A	0.22 ± 0.02^{aA}	0.21 ± 0.02^{aA}	0.14 ± 0.03^{aA}	0.14 ± 0.03^{aA}	0.17 ± 0.03^{aA}	0.17 ± 0.03^{aA}	0.20 ± 0.02^{aA}
B	0.23 ± 0.04^{aA}	0.30 ± 0.04^{bA}	0.55 ± 0.12^{aB}	0.56 ± 0.14^{cB}	0.61 ± 0.05^{cB}	0.57 ± 0.05^{bB}	0.54 ± 0.08^{bB}
C	0.25 ± 0.01^{aBC}	0.20 ± 0.01^{aAB}	0.18 ± 0.03^{bA}	0.28 ± 0.01^{bC}	0.31 ± 0.09^{bC}	0.53 ± 0.06^{bC}	0.54 ± 0.02^{bC}

[a, b, c] Means bearing superscript in a row indicates significant difference (P<0.001) in the absorbance values of particular graft for different time intervals, and [A, B, C,] Means bearing different superscript in a column indicates the significant difference (P<0.05) in the absorbance values at the same time intervals of particular graft

Lymphocyte stimulation test

Protein estimation

The estimated protein levels in the native bone, SDS, and freeze/thaw groups were 2.5, 1.8, and 0.6 (mg/ml) respectively.

The animals of groups B and C showed increased lymphocyte proliferation at all sampling times as compared to their respective values of native antigens. In group B, the acellular antigen increased significantly on the 22nd, 42nd, and 62nd days as compared to 0 day (P<0.05). Whereas in the group C, the acellular antigen increased significantly only on 22nd day (P<0.05) but the values declined thereafter significantly on the 42nd (P<0.05) and 62nd days (Table 4).

Indirect ELISA

The anti-graft antibodies are expressed as mean±SD absorbance at 450 nm wavelength (OD 450) for 30, 60, and 90th days and presented in Table 5.

In group A (autograft) mean±SD absorbance value remained unchanged throughout the period, suggesting the absence of antibodies against native antigens. In group B, the significant increase in absorbance indicated increased antibody production from day 14 onwards (P<0.001) and continued to be elevated even up to 82 days of the observation period. However, group C animals did not show any significant increase in absorbance up to 42 days. It increased significantly on day 62 and remained so even on day 82 (P<0.001).

Comparison between the groups at different time intervals revealed that the animals in the group B showed a significantly higher antibody titer (P<0.05) from the 14th up to the 42nd days as compared to group C. Changes in the absorbance of group C animals closely followed the observation of group A up to 42nd day.

Discussion

The repair and regeneration of large bony defects, secondary to trauma, tumor resection or non union still represent an unsolved problem in veterinary patients. To enhance the healing, the gap can be filled with bone grafts. However, the main clinical problems in the bone graft are osteoclastic resorption, bone remodeling, and long-term stability (Udehiya *et al*., 2013). So, the current effort was made to prepare decellularized bone grafts, which may provide osteoinductive growth factors, mechanical stability, and biologically degradable scaffold without eliciting host immune response to make them suitable biomaterial for bone healing.

The result of the study also correlated with the well-known fact that SDS is an ionic detergent that efficiently solubilizes nuclear and cytoplasmic membranes (Woodsand Gratzer, 2005). At a concentration of 1%, SDS was able to remove most cells, but some cells and nuclear contents remained which was revealed by DNA quantification. The preservation of collagen and GAG content as well as maintaining tensile stiffness makes the tissue stronger, a similar increase in tensile strength was noticed in articular cartilage (Soltz and Ateshian, 2000). However, the presence of few cells and DNA content in the SDS treated graft showed the inefficiency of decellularization which correlated with another study using 2% SDS treated with 4 or 8 h on the facet joint cartilage resulted in complete histological decellularization, but it does not result in the complete elimination of DNA (Elder *et al*., 2009). Several commercially available ECMs show some measurable amount of DNA and even the presence of nuclear material demonstrated in histological staining (Gilbert *et al*., 2008). Further, the SEM results of group B showed that the collagen fibers were more closely packed and disorganized from their orientation as compared to native bone. Sullivian *et al*. (2012) observed that SDS has a tendency to cause disruption of collagen and native tissue structure.

The rapid freeze and thaw method resulted in complete decellularization in the histological examination, as well as reduced DNA content. However, this treatment also preserved collagen, reduced GAG, and retained tensile and compression stiffness (Teo *et al*., 2011). A similar reduction in GAG and minimal DNA content was reported in fibrocartilage treated with a rapid

freeze-thaw cycle (Guo *et al*., 2015). In order to improve the cell adhesion in the decellularized bone, GAG has to be removed. The presence of proteoglycans in the cartilage tissue inhibits cell adhesion, so the removal of GAG was advised to improve cell adhesion in cartilage tissue (Elsaesser *et al*., 2014). Rapid freezing and thawing may disrupt the cell membrane which causes the lysis of cells and fragmentation of cell content by forming intracellular ice crystals. Yet, the devitalized cells were not removed from the graft which was further removed by enzymatic treatment. Temperature variation may disrupt the ECM which can be prevented by controlling the rate of temperature change and duration of treatment (Lehr *et al*., 2011). A single freeze-thaw cycle can effectively prevent the aggregation of leukocytes in bone grafts thereby reducing adverse immune responses and zygomatic reconstruction graft highly integrated with host bone (Karalashvili *et al*., 2017). Multiple freeze-thaw cycles may be used during decellularization which is the most classical treatment for cell lysis (Xing *et al*., 2015). The effect of rapid freeze-thaw processing on tensile, compressive modulus, and mineral density is minimal as compared to untreated bone cylinders (Borchers *et al*., 1995). Finally, on SEM examination, there were no significant changes in collagen fibers which were regular and less disordered from the native bone. It is well documented that using a rapid freeze and thaw cycle on the nucleus pulposus, collagen fibers were regularly arranged flatly packed compared to native bone (Chan *et al*., 2013).

In the current study, bone healing was more evident in group C and partial in group B. Reduction of gap exclusively occurred due to osteoconduction from the cut end of the bone site and lunar surface. The central area of the defect and implant material does not involve any part of the healing process which was confirmed by radiographic and histopathological observations. This implies that bone healing was not brought by osteoinduction. A similar reduction in gap defect size by applying seeded bovine demineralized bone matrix (DBM) has been reported by Caporali *et al*. (2006). Resorption of bone-implant was from all the sites which were gradually replaced by detectable newly grown bone in the present study, and this finding was correlated with the other studies (Nandi *et al*., 2008; Lee *et al*., 2016). In an ideal osteoconduction process, original graft materials should be ultimately substituted with newly formed bone, in the later course of time the original graft is resorbed during the healing process (Yildirim *et al*., 2001). This reflects that the remodeling and resorption rate in group B was slower than the group C. The immunological reactions of the implant may occur due to the aggregation of inflammatory cells around the xenogenic matrix of group B, which may inhibit the osteoconduction and osteoinductive properties of the scaffolds. This might have been a reason for the formation of more fibrous tissue and lesser healing in group B. No host immune response was elicited by decellularized bone placed in an 11 mm critical radial defect of rabbit for 4-8 weeks due to the presence of lesser DNA content (Ventura *et al*., 2016). The presence of DNA content in decellularized tissue indirectly implied the number of cells present in the tissue (Badylak *et al*., 2008). In the present study, the amount of DNA content was significantly diminished, so no immune reaction was elicited. The formation of new bone is started with the infiltration of osteogenic progenitor cells into the extracellular matrix presence of fibronectin on the surface of the matrix allows attaching the cells over the matrix (Cheng *et al*., 2014). Extract of DBM proteins possesses chemotactic and mitogenic activity which has been reported by Somerman *et al*. (1983). However, the proteins which are present in the ECM enhance the chondroblastic differentiation of mesenchymal cells to support the new bone formation by endochondral ossifications (Peng *et al*., 2011). The xenograft which was prepared from freeze and thaw protocols would probably have conserved the ECM osteogenic proteins since it was devoid of chemical treatments. In this study, it was found that bone healing due to group C did not have a significant difference from group A but it significantly scored higher than group B on histopathological evaluation.

The increased level of antigraft antibodies and aggregation of neutrophils at the implanted site in group B could be due to inefficient decellularization as many cells could be seen in histological examination and also DNA quantification. This confirmed the findings of Zheng *et al*. (2005) who proposed that the presence of xenogenic DNA within biological scaffold material has been suggested as a possible cause of the inflammatory response. In another study by Elder *et al*. (2010), it was found that the facet articular cartilage on decellularization with 2% SDS for 8 h achieved complete histological decellularization but the remnant DNA was found to be 60%. It is interesting to note that in this study bone was used which is still harder tissue than cartilage and the concentration of SDS used was 1% which probably involves further investigation into the concentration of SDS on the extent of decellularization. The materials which are used in the living tissue should be biocompatible in order to avoid adverse effects (You *et al*., 2018). *In vivo* lymphocyte proliferation and ELISA represent the identification of the biocompatibility of ideal material. The immunogenic assay revealed that the animals in group B elicit an immune response from day 22 to 82. This may be because of inefficient decellularization by non-ionic detergents. The cell impurities present in the bone scaffold may induce an immune reaction (Ma *et al*., 2013). In their work, the authors evidenced that, SDS treated decellularised bone matrix reduced the growth of rat mesenchymal stem cells. Further, our histological findings revealed that group B animals showed more amount of inflammatory cells on days 30 and 60. The animals of group B showed severe necrosis and fibrous tissue surrounding the implant. Comparison between groups showed that group C does not elicit any local inflammatory reactions but it had slight lymphocyte proliferation and antibody production which was at basal

level up to the 42nd day postoperatively (Gardin *et al*., 2015). Bovine bone decellularized with the freeze and thaw method resulted in less cytotoxicity and biocompatibility in a sheep model in the study performed by Gardin *et al*. (2015).

This study demonstrated that the rapid freeze and thaw method is more promising than the SDS method. The rapid freeze and thaw method is an easy and quick method for the decellularization of bovine cancellous bone along with the preservation of biomechanical and ultrastructural properties and lesser DNA content of the tissue. In the present study, the rapid freeze and thaw group was clinically superior in healing with osteoconductive properties and reduced antigenicity in rabbits. The 1% SDS-treated bones did not result in complete decellularization but maintained the tensile stiffness and had lesser shock-absorbing capacity. Further, in the *in-vivo* application, the SDS group was inferior to the freeze and thaw group as evidenced by lesser healing and aggregation of inflammatory cells. Future studies are needed to investigate the long-term effect of freeze and thaw scaffold on bone healing to determine the use of this implant in various clinical applications.

Acknowledgements

The authors are highly thankful to the Director of Indian Veterinary Research Institute, Izatnagar for providing the facility to carry out this research and also highly acknowledged the DBT(BT/PR1167/MED/32/172/2011), Ministry of Science and Technology, Government of India for providing fund.

Conflict of interest

All authors have declared no conflicts of interest.

References

Amarpal; Kinjavdekar, P; Aithal, HP; Pawde, AM and Pratap, K (2010). Evaluation of Xylazine, Acepromazine and Medetomidine with Ketamine for general anesthesia in rabbits. Scand. J. Lab. Anim. Sci., 37: 223-229.

Badylak, SF; Taylor, D and Uygun, K (2011). Whole-organ tissue engineering: decellularization and recellularization of three-dimensional matrix scaffolds. Annu. Rev. Biomed. Eng., 13: 27-53.

Badylak, SF; Valentin, JE; Ravindra, AK; McCabe, GP and Stewart-Akers, AM (2008). Macrophage phenotype as a determinant of biologic scaffold remodeling. Tissue Eng. Part A., 14: 1835-1842.

Borchers, RE; Gibson, LJ; Burchardt, H and Hayes, WC (1995). Effects of selected thermal variables on the mechanical properties of trabecular bone. Biomaterials. 16: 545-551.

Caporali, EHG; Sheila, CR; Morceli, J; Taga, R; Mauro, JO; Tania, GM; Maria, C; Mamprim, J and Mariana, AC (2006). Assessment of bovine biomaterials containing bone morphogenetic proteins bound to absorbable hydroxyapatite in rabbit segmental bone defects. Acta. Cir. Bras., 21: 367-373.

Chan, LK; Leung, VY; Tam, V; Lu, WW; Sze, KY and Cheung, KM (2013). Decellularized bovine intervertebral disc as a natural scaffold for xenogenic cell studies. Acta. Biomater., 9: 5262-5272.

Cheng, CW; Solorio, LD and Alsberg, E (2014). Decellularized tissue and cell-derived extracellular matrices as scaffolds for orthopaedic tissue engineering. Biotechnol. Adv., 32: 462-484.

Elder, BD; Eleswarapu, SV and Athanasiou, KA (2009). Extraction techniques for the decellularization of tissue engineered articular cartilage constructs. Biomaterials. 30: 3749-3756.

Elder, BD; Kim, DH and Athanasiou, KA (2010). Developing an articular cartilage decellularization process toward facet joint cartilage replacement. Neurosurgery. 66: 722-727.

Elsaesser, AF; Bermueller, C; Schwarz, S; Koerber, L; Breiter, R and Rotter, N (2014). *In vitro* cytotoxicity and *in vivo* effects of a decellularized xenogeneic collagen scaffold in nasal cartilage repair. Tissue Eng. Part A., 20: 1668-1678.

Frohlich, M; Grayson, WL; Marolt, D; Gimble, JM; Kregar-Velikonja, N and Vunjak-Novakovic, G (2010). Bone grafts engineered from human adipose-derived stem cells in perfusion bioreactor culture. Tissue Eng. Part A., 16: 179-189.

Gardin, C; Ricci, S; Ferroni, L; Guazzo, R; Sbricoli, L; De Benedictis, G; Finotti, L; Isola, M; Bressan, E and Zavan, B (2015). Decellularization and delipidation protocols of bovine bone and pericardium for bone grafting and guided bone regeneration procedures. PLoS One. 10: e0132344.

Gilbert, TW; Freund, J and Badylak, SF (2009). Quantification of DNA in biological scaffold materials. J. Surg. Res., 152: 135-139.

Gock, H; Murray-Segal, L; Salvaris, E; Cowan, PD and Apice, AJ (2004). Allogeneic sensitization is more effective than xenogeneic sensitization in eliciting Gal-mediated skin graft rejection. Transplantation. 77: 751-753.

Guo, L; Qu, J; Zheng, C; Cao, Y; Zhang, T; Lu, H and Hu, J (2015). Preparation and characterization of a novel decellularized fibrocartilage "book" scaffold for use in tissue engineering. PLoS One. 4: e0144240.

Heiple, KG; Goldberg, VM; Powell, AE; Bos, GD and Zika, JM (1987). Biology of cancellous bone grafts. Orthop. Clin. North. Am., 18: 179-185.

Jonitz, A; Lochner, K; Lindner, T; Hansmann, D; Marrot, A and Bader, R (2011). Oxygen consumption, acidification and migration capacity of human primary osteoblasts within a three-dimensional tantalum scaffold. J. Mater. Sci. Mater. Med., 22: 2089-2095.

Kalab, M; Karkoska, J; Kaminek, M and Santavy, P (2015). Successful three-year outcome in a patient with allogenous sternal bone graft in the treatment of massive post-sternotomy defects. Int. J. Surg. Case Rep., 7: 6-9.

Karalashvili, L; Chichua, N; Menabde, G; Atskvereli, L and Grdzelidze, T (2017). Decellularized bovine bone graft for zygomatic bone reconstruction. Med. Case Rep., 4: 1-5.

Kruisbeek, AM; Shevach, E and Thornton, AM (2004). Proliferative assays for T cell function. Curr. Protoc. Immunol., 60: 3-12.

Lane, JM and Sandhu, HS (1987). Current approach to experimental bone grafting. Orthop. Clin. North Am., 18: 213-225.

Lee, DJ; Diachina, S; Lee, YT; Zhao, L; Zou, R; Tang, N;

Han, H; Chen, X and Ko, CC (2016). Decellularized bone matrix grafts for calvaria regeneration. J. Tissue Eng., 7: 1-11.

Lehr, EJ; Rayat, GR; Chiu, B; Churchill, T; McGann, LE and Coe, JY (2011). Decellularization reduces immunogenicity of sheep pulmonary artery vascular patches. J. Thorac. Cardiovasc. Surg., 141: 1056-1062.

Ma, R; Li, M; Luo, J; Yu, H; Sun, Y; Cheng, S and Cui, P (2013). Structural integrity, ECM components and immunogenicity of decellularized laryngeal scaffold with preserved cartilage. Biomaterials. 34: 1790-1798.

Mollon, B; Kandel, R; Chahal, J and Theodoropoulos, J (2013). The clinical status of cartilage tissue regeneration in humans. Osteoarthr. Cartil., 21: 1824-1833.

Nandi, SK; Kundu, B; Ghosh, SK; De, DK and Basu, D (2008). Efficacy of nano-hydroxyapatite prepared by an aqueous solution combustion technique in healing bone defects of goat. J. Vet. Sci., 9: 183-191.

Oryan, A; Alidadi, S; Moshiri, A and Maffulli, N (2014). Bone regenerative medicine: classic options, novel strategies, and future directions. J. Orthop. Surg. Res., 9: 1-27.

Peng, F; Yu, X and Wei, M (2011). *In vitro* cell performance on hydroxyapatite particles/poly (L-lactic acid) nanofibrous scaffolds with an excellent particle along nanofiber orientation. Acta. Biomater., 7: 2585-2592.

Quan, TM; Vu, DN; My, NT and Ha, TL (2014). Decellularization of xenogenic bone grafts for potential use as tissue engineering scaffolds. Int. J. Life Sci. Med. Res., 4: 38-45.

Remya, V; Kumar, N; Sharma, AK; Mathew, DD; Negi, M; Maiti, SK; Shrivastava, S and Kurade, NP (2014). Bone marrow derived cell-seeded extracellular matrix: A novel biomaterial in the field of wound management. Vet. World. 7: 1019-1025.

Sambrook, J and Russell, DW (2001). *Molecular cloning- a laboratory manual*. 3rd Edn., New York, Cold Spring Harbor Laboratories Press, Cold Spring Harbor.

Soltz, MA and Ateshian, GA (2000). A conewise linear elasticity mixture model for the analysis of tension-compression nonlinearity in articular cartilage. J. Biomech. Eng., 122: 576-586.

Somerman, M; Hewitt, AT; Varner, HH; Schiffmann, E; Termine, J and Reddi, AH (1983). Identification of a bone matrix-derived chemotactic factor. Calcif. Tissue Internat., 35: 481-485.

Stievano, D; Di Stefano, A; Ludovichetti, M; Pagnutti, S; Gazzola, F; Boato, C and Stellini, E (2008). Maxillary sinus lift through heterologous bone grafts and simultaneous acid-etched implants placement. Minerva. Chir., 63: 79-91.

Sullivan, DC; Mirmalek-Sani, SH; Deegan, DB; Baptista, PM; Aboushwareb, T; Atala, A and Yoo, JJ (2012). Decellularization methods of porcine kidneys for whole organ engineering using a high-throughput system. Biomaterials. 33: 7756-7764.

Teo, KY; DeHoyos, TO; Dutton, JC; Grinnell, F and Han, B (2011). Effects of freezing-induced cell-fluid-matrix interactions on the cells and extracellular matrix of engineered tissues. Biomaterials. 32: 5380-5390.

Udehiya, RK; Aithal, HP; Kinjavdekar, P; Pawde, AM; Singh, R and Sharma, GT (2013). Comparison of autogenic and allogenic bone marrow derived mesenchymal stem cells for repair of segmental bone defects in rabbits. Vet. Sci. Res. J., 94: 743-752.

Ventura, R; Padalhin, A; Young-Ki, M and Byong-Taek, L (2016). Bone regeneration of decellularized *in-vivo* deposited extracellular matrix (ECM) on hydroxyapatite sponge scaffold. MOJ Cell Sci. Rep., 3: 3-6.

Woods, T and Gratzer, PF (2005). Effectiveness of three extraction techniques in the development of a decellularized bone-anterior cruciate ligament bone graft. Biomaterials. 26: 7339-7349.

Xing, Q; Yates, K; Tahtinen, M; Shearier, E; Qian, Z and Zhao, F (2015). Decellularization of fibroblast cell sheets for natural extracellular matrix scaffold preparation. Tissue Eng. Part C Methods. 21: 77-87.

Yildirim, M; Spiekermann, H; Handt, S and Edelhoff, D (2001). Maxillary sinus augmentation with the xenograft Bio-Oss® and autogenous intraoral bone for qualitative improvement of the implant site: a histologic and histomorphometric clinical study in humans. Int. J. Oral Maxillo Fac. Implants. 16: 23-33.

You, L; Weikang, X; Lifeng, Y; Changyan, L; Yongliang, L; Xiaohui, W and Bin, X (2018). *In vivo* immunogenicity of bovine bone removed by a novel decellularization protocol based on supercritical carbon dioxide. Artif. Cells Nanomed. Biotechnol., 5: 334-344.

Zheng, MH; Chen, J; Kirilak, Y; Willers, C; Xu, J and Wood, D (2005). Porcine small intestine submucosa (SIS) is not an acellular collagenous matrix and contains porcine DNA: possible implications in human implantation. J. Biomed. Mater. Res. B Appl. Biomater., 73: 61-67.